NANO LETTERS

Letter

pubs.acs.org/NanoLett

Nanophotonic Enhancement of the Förster Resonance Energy-Transfer Rate with Single Nanoapertures

Petru Ghenuche, Juan de Torres, Satish Babu Moparthi, Victor Grigoriev, and Jérôme Wenger*

CNRS, Aix-Marseille Université, Centrale Marseille, Institut Fresnel, UMR 7249, 13013 Marseille, France

Supporting Information

ABSTRACT: Tailoring the light−matter interaction and the local density of optical states (LDOS) with nanophotonics provides accurate control over the luminescence properties of a single quantum emitter. This paradigm is also highly attractive to enhance the near-field Förster resonance energy transfer (FRET) between two fluorescent emitters. Despite the wide applications of FRET in nanosciences, using nanophotonics to enhance FRET has remained a debated and complex challenge. Here we demonstrate enhanced energy transfer within single donor−acceptor fluorophore pairs confined in single gold nanoapertures. Experiments monitoring both the donor and the acceptor emission photodynamics clearly establish a linear dependence of the FRET rate on the LDOS in nanoapertures, demonstrating that nanophotonics can be used to intensify the near-field energy transfer. Strikingly, we observe a significant six-fold increase in the FRET rate for large donor−acceptor separations exceeding 13 nm. Exciting opportunities are opened to investigate biochemical structures with donor−acceptor distances much beyond the classical Förster radius. Importantly, our approach is fully compatible with the detection of single biomolecules freely diffusing in water solution under physiological conditions.

KEYWORDS: *FRET, plasmonics, LDOS, metal nanoaperture, zero mode waveguide, fluorescence enhancement*

Nanoscale energy transfer between molecules is a core phenomenon in photosynthesis[1−3] and an enabling technology for photovoltaics,[4,5] organic lighting sources,[6] or biosensing.[7] When the distance between the excited donor D to the ground-state acceptor molecule A is on the range of 2−20 nm, the energy transfer is adequately described by the Förster resonance energy-transfer (FRET) formalism, which accounts for near-field nonradiative dipole−dipole interaction.[8] As the FRET efficiency goes down with the inverse sixth power of the D−A distance, FRET provides accurate information with subnanometer resolution on the spatial relationship between two fluorophore-labeled sites in biological structures.[9] FRET has thus become one of the most popular tools in single-molecule spectroscopy and is largely used to study conformational changes in macromolecules as well as molecular interaction dynamics between proteins, DNA, RNA, and peptide molecules.[10,11]

The interaction between molecules and light on the nanoscale is at the heart of FRET. Therefore, using nanophotonics to control light at the nanoscale is appealing to enhance the near-field dipole−dipole energy transfer. Since the pioneering works of Purcell and Drexhage,[12,13] it is well established that the luminescence properties of a single quantum emitter can be engineered by its photonic environment through the local density of optical states (LDOS).[14,15] Successful demonstrations of this concept include cavity quantum electrodynamics,[16] photonic band gap materials,[17,18] and more recently plasmonic antennas.[19,20] However, when the discussion turns to the interaction of two emitters with their environment, the LDOS influence on the Förster energy transfer remains a debated question. Because FRET directly competes with the donor direct emission and the donor nonradiative energy losses to its environment, it is unclear whether Förster transfer can be enhanced when the LDOS is tuned to increase the donor emission. Despite the important use of FRET in single-molecule biophysics, experiments quantifying the influence of the photonic environment on the FRET rate are scarce. Pioneering works on ensemble measurements in microcavities suggested that the FRET rate depends *linearly* on the donor emission rate and the LDOS.[21−24] However, the concentration of the dye layers was so high that self-quenching was dominant, and no information could be obtained from acceptor emission. While several theoretical works were proposed to support the LDOS dependence of FRET,[25−29] it was also suggested that the FRET rate was quadratically dependent on the LDOS[30] or even independent of the LDOS.[31] A recent experimental study on molecules near a planar mirror concludes that the energy-

Received: May 15, 2014
Revised: July 10, 2014
Published: July 14, 2014

transfer rate is independent of the LDOS,[32] in agreement with the general theory developed therein. It has also been reported recently that the FRET rate cannot be increased by increasing the solvent's refractive index.[33] Several other studies have considered the use of nanophotonics in combination with FRET but without quantifying the LDOS influence on the FRET process.[34−44] Given this wide interest and the presence of contradicting theories, we believe a clear experimental quantification is necessary to clarify the influence of the photonic environment on the FRET process. Moreover, we also point out that most studies consider only the donor emission photodynamics and measure ensembles of molecules, while ideally experiments should be conducted at the single-molecule level by monitoring both the donor and acceptor emission photodynamics.

Here we explore the LDOS influence on the FRET process using precisely defined plasmonic nanoapertures to control the LDOS and single donor−acceptor fluorophore pairs on double-stranded DNA linkers to provide a wide range of FRET rates and efficiencies (Figure 1a). To avoid any ambiguity, our experiments monitor single molecule diffusing events and record both the donor and the acceptor emission photodynamics. Importantly for biophotonic applications, our approach is fully compatible with the detection of single biomolecules freely diffusing in water solution at physiological concentrations of several micromolar. Two separate measurements of the FRET rate Γ_{FRET} and efficiency E_{FRET} are obtained based either on the donor lifetime reduction in the presence of the acceptor or the acceptor fluorescence increase in the presence of the donor. The FRET efficiency is defined as the probability of energy transfer over all donor transition events: $E_{FRET} = \Gamma_{FRET}/\Gamma_{DA} = \Gamma_{FRET}/(\Gamma_{FRET} + \Gamma_D)$, where $\Gamma_D = \Gamma_{D,rad} + \Gamma_{D,nonr}$ is the total decay rate of the isolated donor (without acceptor, accounting for both radiative and nonradiative transitions) and $\Gamma_{DA} = \Gamma_D + \Gamma_{FRET}$ is the total decay rate of the donor in the presence of the acceptor. Following the common approach in plasmonics, we define the LDOS as the number of modes per unit volume and frequency at the position of the dipole emitter, where the energy can be released during the spontaneous emission process.[14] The energy release can occur by radiating a photon in the far field or by local absorption (ohmic losses) into the metal. Therefore, this definition of LDOS encompasses both radiative and nonradiative transitions. With this definition, the LDOS is always proportional to the donor total decay rate Γ_D (inverse of the fluorescence lifetime).

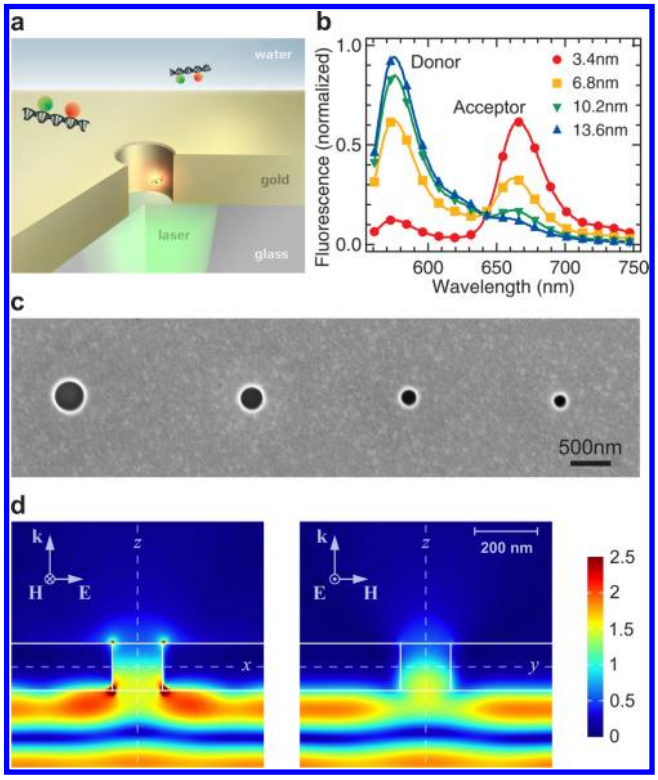

Figure 1. Single-molecule FRET in a gold nanoaperture. (a) Schematic of a donor−acceptor pair on a DNA molecule diffusing inside and around a single nanoaperture milled in a gold film on a glass coverslip. (b) Normalized fluorescence emission spectra for different donor−acceptor distances in water solution. Emission of the Atto550 donor at 580 nm is recovered while emission of the Atto647N acceptor at 670 nm vanishes as the donor−acceptor distance is increased from 3.4 to 13.6 nm. (c) Scanning electron microscopy image of nanoapertures of diameters from 380 to 160 nm. (d) Finite-element computation of excitation electric field amplitude enhancement for two orthogonal planes on a gold nanoaperture of 160 nm diameter. The incoming light at a wavelength of 550 nm is polarized along the x axis.

According to Förster theory,[8,14,29] the energy-transfer rate between two dipoles in free space is expressed as $\Gamma_{FRET} = (R_0/R)^6\Gamma_D$, where R_0 is the Förster radius and R is the donor−acceptor distance separation. This formula indicates a linear dependence of the FRET rate with the isolated donor decay rate. It is therefore tempting to generalize and conclude that Γ_{FRET} varies linearly with the LDOS, which is proportional to Γ_D. However, the Förster theory was derived only in the case of a homogeneous photonic environment. The question about the LDOS influence on FRET can be reformulated as to determine whether this formula is still valid in a complex nanophotonic environment.

To provide a wide range of LDOS, we use circular nanoapertures with diameters ranging from 160 to 380 nm milled in a 150 nm thick gold film on a glass coverslip by focused ion beam (Figure 1c,d). Molecules randomly diffusing inside the apertures experience an average fluorescence lifetime reduced by a factor up to three-fold. While the LDOS is expected to vary spatially inside the nanoaperture depending on the position and orientation of the emitter respective to the metal,[45,46] the net fluorescence lifetime reduction observed on the decay traces averaged for all emitter positions and orientations inside the aperture demonstrates an increase in the spatially averaged LDOS inside nanoapertures.[47−49] Nanoapertures thus realize a reproducible platform to tune the spatially averaged LDOS. They also have a broad spectral response so that the same structure can enhance both the donor and the acceptor emission. (See Supporting Information Figures S2 and S3.)

To provide a wide range of FRET rates and efficiencies, we synthesize double-stranded DNA molecules with increasing distances between the Atto550 donor and the Atto647N acceptor from 10 to 40 base pairs (3.4 to 13.6 nm). The double-stranded DNA forms a rigid linker enabling accurate positioning of the donor and acceptor with subnanometer resolution.[50] The spectral overlap between Atto550 and Atto647N ensures Förster transfer with a characteristic distance R_0 of 6.5 nm in pure water medium, which is confirmed by ensemble fluorescence spectroscopy (Figure 1b). Hence by varying either the donor−acceptor distance or the nanoaperture

dx.doi.org/10.1021/nl5018145 | Nano Lett. 2014, 14, 4707−4714

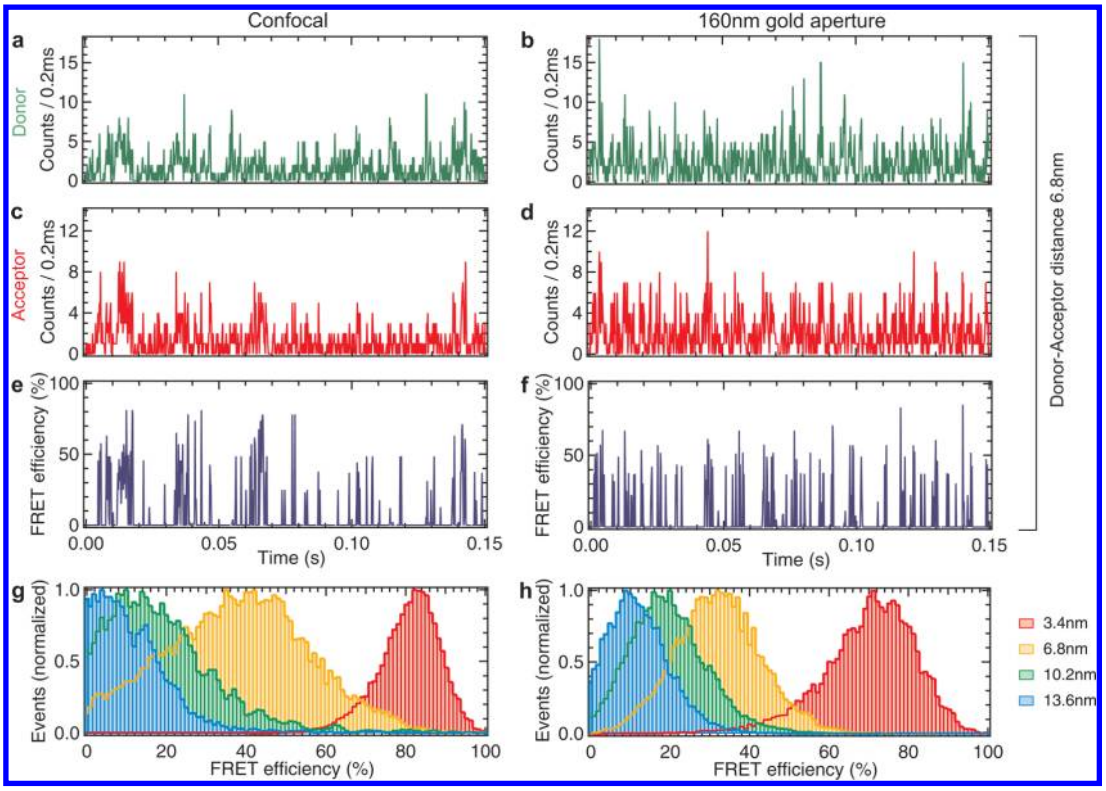

Figure 2. FRET burst analysis of single-molecule diffusion events in a gold nanoaperture. (a–f) Example of time traces for donor–acceptor pairs separated by 6.8 nm (20 base pairs) diffusing in solution and probed by the diffraction-limited confocal microscope (a,c,e) and in a gold nanoaperture of 160 nm diameter (b,d,f). The concentration is set so as to have less than one molecule in the detection volume in each case (confocal 1 nM, nanoaperture 250 nM). For each fluorescence burst exceeding the detection threshold in the donor detection channel (a,b) or the acceptor channel (c,d), a FRET efficiency is calculated (e,f). The binning time is 0.2 ms and the total trace duration is 200 s. (g,h) FRET efficiency histograms extracted from fluorescence burst analysis for different donor–acceptor separations in confocal (g) and in the 160 nm nanoaperture (h).

diameter, we have two independent parameters to tune the FRET rate and the LDOS and monitor the effect of the LDOS on the FRET rate.

For direct observation of single-molecule diffusion events, the nanoaperture sample is covered by a water solution containing the diluted DNA FRET pairs. Every time a fluorescent molecule crosses the detection volume a fluorescence burst is generated, which results in the typical time traces displayed on Figure 2a–d. The burst duration is set by the translational diffusion time and typically amounts to 460 μs for the confocal reference and 135 μs for the nanoaperture of 160 nm diameter. Comparing the bursts intensity in confocal to the nanoaperture, a fluorescence enhancement of about two times is found for the donor and the acceptor detection channels. (See Supporting Information Figures S1 and S2 for fluorescence correlation spectroscopy (FCS) analysis and fluorescence enhancement factors.) For each fluorescence photon burst, a FRET efficiency E_{FRET} can be computed and collected in a histogram (Figure 2e,f). Importantly to avoid errors in the FRET measurement, our analysis carefully takes into account the direct excitation of the acceptor by the laser light, donor emission crosstalk into the acceptor channel, and differences in the quantum yields and detection efficiencies of the donor and acceptor emission. (See the Methods section for details.) Figure 2g,h summarizes the FRET efficiency histograms for increasing donor–acceptor distances in confocal and in the 160 nm nanoaperture. Except for the 3.4 nm D–A distance, the histogram width is reduced by ~50% inside the nanoaperture as compared with confocal reference. This is primarily a consequence of the higher photon counts per emitter (fluorescence enhancement) in the nanoaperture. The average FRET efficiencies in the nanoaperture are affected differently depending on the D–A distance. In the case of the short D–A distance of 3.4 nm, the FRET efficiency is marginally reduced by the nanoaperture from 83 to 76%. On the contrary, the FRET efficiency for the longest D–A distance of 13.6 nm is actually increased significantly from 4 to 10%. This observation appears highly promising to extend the spatial applicability of single molecule FRET beyond the classical Förster range.

To quantify the acceleration of the fluorescence photodynamics and the LDOS enhancement in nanoapertures, we record the donor fluorescence decay traces by time-correlated single photon counting. Figure 3a–c reports the influence of the nanoaperture diameter. (See also Supporting Information Figure S3.) For the isolated donor, the fluorescence lifetime τ_D decreases from 3.7 to 1.3 ns as the nanoaperture diameter is reduced to 160 nm. (See the Methods section for details of the decay trace analysis.) This lifetime reduction is equivalent to an increase in the donor-only total decay rate $\Gamma_D = 1/\tau_D$ and the LDOS by a factor 2.9 (Figure 3c). In the presence of the acceptor at a 6.8 nm separation, the donor emission dynamics are further accelerated by the additional decay channel brought by the acceptor $\Gamma_{DA} = \Gamma_D + \Gamma_{FRET}$, and the donor fluorescence lifetime $\tau_{DA} = 1/\Gamma_{DA}$ is further reduced (Figure 3b). We monitor a lifetime reduction as a function of the aperture diameter similar to the case of the donor only, from 2.5 to 0.9 ns in the presence of the acceptor. Figure 3d–f then describes

dx.doi.org/10.1021/nl5018145 | Nano Lett. 2014, 14, 4707–4714

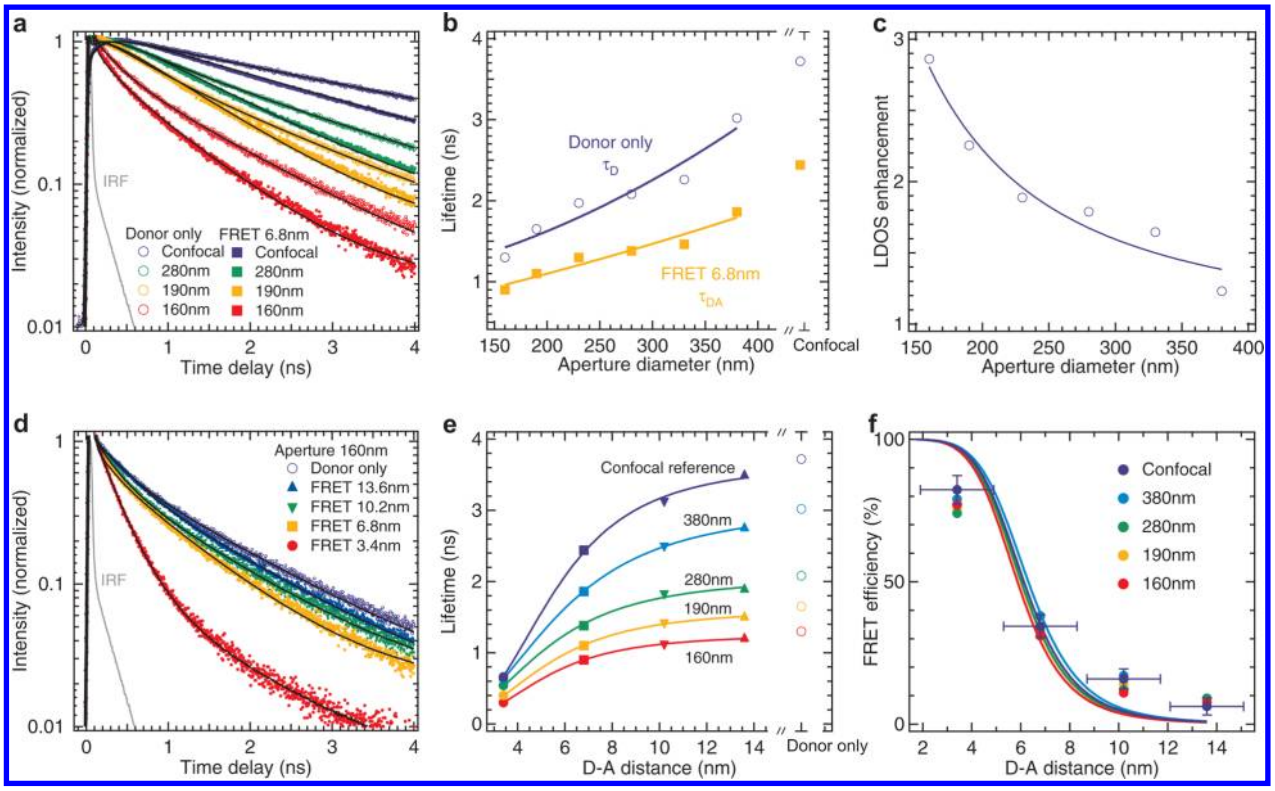

Figure 3. Donor lifetime reduction in nanoapertures. (a) Normalized donor decay traces when no acceptor is present (empty circles) or when the acceptor is separated by 6.8 nm (filled squares). The black lines are numerical fits convoluted by the instrument response function (IRF). From top to bottom, the different colors are associated with the confocal case or with nanoapertures of decreasing diameters from 280 to 160 nm. In each case, the presence of the acceptor induces a significant acceleration of the donor emission dynamics. (b) Donor fluorescence lifetime as a function of the nanoaperture diameter, obtained from the data shown in panel a. (c) LDOS enhancement as a function of the nanoaperture diameter, obtained from the donor-only lifetime reduction as compared with the confocal reference. (d) Normalized donor decay traces in a 160 nm nanoaperture as the acceptor separation is reduced. (e) Donor fluorescence lifetime as a function of the donor−acceptor separation for different nanoaperture diameters and for the confocal reference. For each donor−acceptor distance, a clear reduction of the donor fluorescence lifetime is observed as the nanoaperture diameter is reduced. (f) FRET efficiency deduced from the donor lifetime reduction in the presence of the acceptor, as a function of the donor−acceptor distance R. The lines are numerical fits assuming a $1/R^6$ dependence and random orientation of both donor and acceptor dipole. Vertical error bars indicate one standard deviation, horizontal errors bars assume a 1.5 nm distance uncertainty that we relate to the dye-DNA linker flexibility.

the influence of the donor−acceptor separation for a given nanoaperture diameter. A clear reduction of the donor emission lifetime (donor quenching) is observed as the D−A distance is reduced, with a similar trend observed for all nanoaperture diameters. The decay rates in the presence and absence of the acceptor also enable us to compute the FRET efficiency as $E_{FRET} = \Gamma_{FRET}/(\Gamma_{FRET} + \Gamma_D) = 1 - \Gamma_D/\Gamma_{DA}$ (Figure 3f). As for the analysis based on the fluorescence bursts (Figure 2g,h), we observe that the FRET efficiencies deduced from the decay traces appear marginally affected by the nanoaperture in the case of short D−A separations. The deviation from the standard FRET model seen already for the confocal case stems from steric interactions between the fluorophores and the DNA double strand, which affect the dipole−dipole orientations. Similar behaviors have already been reported for confocal FRET.[51−53]

To establish the effect of the LDOS on the Förster transfer within nanoapertures, we display in Figure 4a,b the FRET rate Γ_{FRET} and efficiency E_{FRET} as a function of the isolated donor total decay rate Γ_D, which is proportional to the LDOS at the donor emission wavelength. A strength of our study is that we use two different approaches to quantify both Γ_{FRET} and E_{FRET} based either on the donor lifetime reduction, or the acceptor fluorescence bursts. (See the Methods.) This provides the first set reported to date of complete experimental evidence down to the single -molecule level. The data points in Figure 4a,b summarize the results: filled markers are deduced from the donor lifetime reduction, and empty markers are deduced from fluorescence burst analysis. Both approaches converge to similar values, confirming the general trend. Our data clearly demonstrate a linear dependence of the FRET rate on the LDOS for all four D−A separations (Figure 4a and Supporting Information Figure S4). This result is further confirmed by the slight variations of the FRET efficiency as the LDOS changes (Figure 4b), which was already observed as a function of the aperture diameter in Figures 2g,h and 3f: the FRET rate Γ_{FRET} must increase accordingly as Γ_D increases to maintain a similar ratio $E_{FRET} = \Gamma_{FRET}/(\Gamma_{FRET} + \Gamma_D)$.

In the current debate about the LDOS influence on FRET,[22,32,33] our work importantly demonstrates that the FRET rate can effectively be tuned by the LDOS in nanoapertures. Our results indicate that the presence of strong field gradients and moderate dissipation losses to the metal are promoting the near-field Förster transfer between distant donor and acceptor by increasing the donor dipole oscillator strength. We point out that our approach fully takes into account the nonradiative decay of the isolated donor to the metal, which in the case of a 160 nm aperture can become as strong as the

dx.doi.org/10.1021/nl5018145 | Nano Lett. 2014, 14, 4707−4714

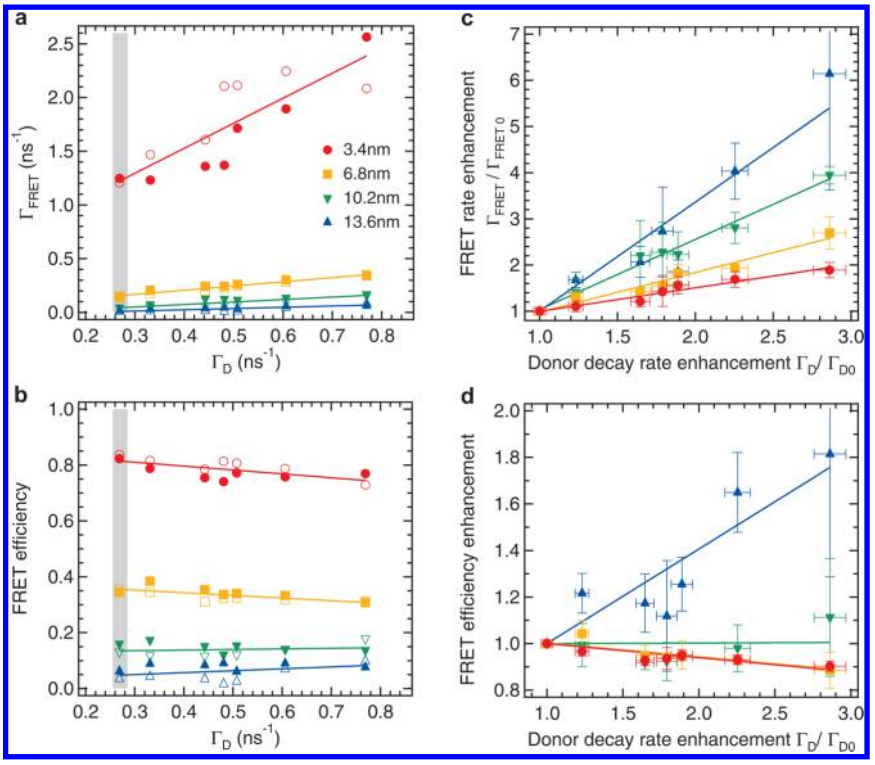

Figure 4. Nanophotonic control of FRET rate and efficiency. (a) FRET rate Γ_{FRET} and (b) FRET efficiency E_{FRET} for different donor−acceptor separations as a function of the isolated donor decay rate Γ_D that is proportional to the LDOS. Filled markers denote the data points deduced from the donor lifetime reduction, while empty markers denote data points deduced from fluorescence burst analysis. The lines are numerical fits of the average FRET rate between the two measurement methods and show a linear dependence of the FRET rate with the isolated donor decay rate for all donor−acceptor separations. The gray shaded region indicates the FRET rates obtained for the confocal reference. The evolution with the LDOS is further evidenced by normalizing the data in panels a and b by the values found for the confocal reference. This results in the graphs in panels c and d representing the normalized enhancement of the FRET rate and efficiency as a function of the normalized enhancement of the donor-only decay rate. Horizontal error bars indicate one standard deviation of the measurements, and vertical error bars are the difference between the two measurement methods for the average FRET rate and efficiency.

radiative transition rate. (See Supporting Information section 5 for a detailed discussion.) For aperture diameters ranging between 150 and 350 nm, the FRET rate is always found to scale as the total decay rate of the isolated donor, including both radiative and nonradiative contributions.

Our experiments contradict the theories leading to the general conclusion that the FRET rate is independent of the LDOS. As compared with previous work near a planar mirror,[32] we believe that the different D−A separations, the brighter emission rates, and the larger LDOS variations in nanoapertures further emphasize experimentally the LDOS influence on the FRET process. For a purely homogeneous environment, it was recently shown that increasing the solvent's refractive index did not enhance the FRET rate despite a reduced donor lifetime.[33] In contrast, our work fully exploits the nanophotonic effects offered by the aperture cavity to tune the LDOS.

To go further into the analysis, we compute the FRET rate enhancement $\Gamma_{FRET}/\Gamma_{FRET0}$ as a function of the LDOS enhancement Γ_D/Γ_{D0}. To do this, we normalize the results in Figure 4a,b with the values found for the confocal reference (Γ_{FRET0}, Γ_{D0}). This representation reveals better the effect of the LDOS for the cases of large D−A separations and weak FRET rates and efficiencies. The global trend observed is a larger enhancement of the FRET rate as the D−A distance is increased: typically a two times enhancement of the FRET rate is observed for a D−A distance of 3.4 nm and a 160 nm aperture, whereas the FRET rate enhancement can be as large as six times when the D−A distance is 13.6 nm. The FRET rate enhancement dependence on the donor−acceptor distance can be explained by the fact that the observed FRET rate within a nanoaperture is a sum of contributions from different nonradiative energy-transfer channels: the direct (dipole−dipole) transfer, the energy transfer mediated by the nanoaperture, and possibly an interference term accounting for the phase shift between these two channels.[28] We expect the direct dipole−dipole transfer to be dominant at short D−A separations, while the nonradiative energy transfer mediated by the nanoaperture can have a more pronounced effect for large D−A separations. Disentangling these contributions is still an experimental challenge; our data is a first step in revealing this phenomenon. Importantly for biophysical applications of FRET at large D−A separations, this six-fold increase in the FRET rate is accompanied by a nearly doubling of the FRET efficiency. This observation offers exciting opportunities to explore a new domain for single molecule FRET beyond the classical 8−10 nm Förster range.

Monitoring the fluorescence bursts from single molecules allows us to recover the complete statistical distribution of the FRET rates. This is obtained by reformulating the formula defining the FRET efficiency $\Gamma_{FRET} = \Gamma_D E_{FRET}/(1 - E_{FRET})$ and using the separate measurements of the FRET efficiency histograms (Figure 2h) and the donor-only decay rates Γ_D (Figure 3b). Figure 5 depicts the distribution of the measured FRET rates enhancement $\Gamma_{FRET}/\langle\Gamma_{FRET0}\rangle$, where $\langle\Gamma_{FRET0}\rangle$ is

dx.doi.org/10.1021/nl5018145 | *Nano Lett.* 2014, 14, 4707−4714

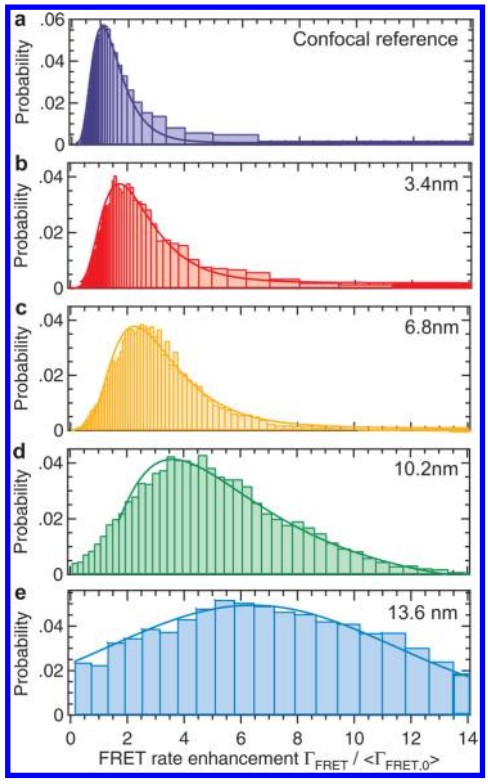

Figure 5. Distribution of FRET rates in nanoapertures as compared with the average FRET rate found in the confocal reference. The histograms in panel a is the confocal reference for a 3.4 nm donor−acceptor separation, while data in panels b−e were taken in a 160 nm gold nanoaperture with increasing donor−acceptor distances. Lines are numerical fits with a log-normal distribution.

the average FRET rate found for the confocal reference. As for Figure 4c, the global trend is a larger enhancement of the FRET rate as the D−A distance increases. Furthermore, the statistical distributions show that significant FRET rate enhancement above five-fold is reproducibly observed, demonstrating that nanophotonics can be used to enhance the near-field energy transfer.

In summary, we report enhanced energy transfer within single donor−acceptor fluorophore pairs confined in gold nanoapertures and demonstrate experimentally that the Förster energy-transfer rate depends linearly on the LDOS. To provide a complete picture of FRET in single nanoapertures, we conduct all of our experiments on well-defined single donor−acceptor pairs and monitor all photodynamics observables on both the donor and the acceptor emission. By increasing the donor dipole oscillator strength, the nanoaperture allows us to efficiently transfer the energy to the acceptor dipole in the near-field. These findings are important because they unlock the potential application of the large nanophotonic toolbox for single emitter fluorescence control to further enhance the FRET process broadly used in single-molecule spectroscopy applied to life sciences. In particular, we observe a significant six-fold increase in the FRET rate for large donor−acceptor separations exceeding 13 nm. This result opens exciting opportunities to investigate biochemical structures with donor−acceptor distances much beyond the classical Förster radius. An additional advantage is brought by the compatibility of our approach with the detection of single biomolecules freely diffusing in water solution under physiological conditions,[44,54−56] providing a new class of substrates for enhanced single-molecule FRET analysis.

Methods. Nanoaperture Sample Fabrication. Nanoapertures are milled by focused ion beam (FEI Strata Dual Beam 235) on 150 nm thick gold films deposited using thermal evaporation on standard 150 μm thick glass coverslips.

DNA Synthesis and Preparation. Double-stranded DNA constructs of 51 base pairs length are designed with a one donor label Atto550 on the forward strand and one acceptor label Atto647N on the reverse strand, at varying distances, so that the donor and acceptor are separated by 10, 20, 30, or 40 base pairs from each other to make 3.4, 6.8, 10.2, or 13.6 nm varying distance, respectively. As 10 base pairs make a complete turn on the DNA double strand, the choice of D−A separation as multiples of 10 base pairs avoids taking into account the complex 3-D structure of DNA to estimate the D−A distance.[50] All constructs are purchased from IBA, Goettingen, Germany.

The forward strand sequence is 5′ CCTGAGCGTACT-GCAGGATAGCCTATCGCGTGTCATATGCTGTT$\mathbf{T}_{D}$-CAGTGCG 3′. The reverse strand sequence is 5′ CGCA-CTGAACAGCATAT$\mathbf{T}_{10}$GACACGCGA$\mathbf{T}_{20}$AGGCTATCC-$\mathbf{T}_{30}$GCAGTACGC$\mathbf{T}_{40}$CAGG 3′.

The donor-only and acceptor-only references are constructed with the same sequences by replacing either the acceptor or the donor with unlabeled complementary strand, respectively. The strands are annealed at 10 μM concentration in 20 mM Tris, 1 mM EDTA, 500 mM NaCl, and 12 mM $MgCl_2$ buffer and by heating to 95 °C for 5 min followed by slow cooling to room temperature. Samples were then stored at −28 °C. For single-molecule experiments labeled double-stranded DNA, stocks are diluted in a 10 mM Hepes-NaOH buffer, pH 7.5 (Sigma-Aldrich).

Experimental Setup. The experimental setup is based on a confocal inverted microscope with a Zeiss C-Apochromat 63× 1.2NA water-immersion objective. The excitation source is a iChrome-TVIS laser (Toptica) delivering 3 ps pulses at 40 MHz repetition rate and 550 nm wavelength. Filtering the laser excitation is performed by a set of two bandpass filters (Chroma ET525/70 M and Semrock FF01-550/88). The excitation power at the diffraction limited spot is set to 40 μW for all experiments. Positioning the nanoaperture at the laser focus spot is obtained with a multiaxis piezoelectric stage (Polytech PI P-517.3CD). Dichroic mirrors (Chroma ZT594RDC and ZT633RDC) separate the donor and acceptor fluorescence light from the epi-reflected laser and elastically scattered light. The detection is performed by two avalanche photodiodes (Micro Photon Devices MPD-5CTC with 50 μm active surface and <50 ps timing jitter) with 620 ± 20 nm (Chroma ET605/70 M and ET632/60M) and 670 ± 20 nm (Semrock FF01-676/37) fluorescence bandpass filters for the donor and acceptor channels, respectively. The photodiode signal is recorded by a fast time-correlated single photon counting module (Hydraharp400, Picoquant) in time-tagged time-resolved (TTTR) mode. The temporal resolution of our setup for fluorescence lifetime measurements (width of the instrument response function) is 37 ps at half-maximum.

FRET Analysis Based on Donor Lifetime. All decay traces are analyzed using the commercial software Symphotime 64 (Picoquant), taking into account the reconvolution by the instrument response function (IRF). The time interval for fit is truncated so that more than 85% of the detected photons fall into the region of interest to maximize the signal-to-noise ratio. As shown already in some of our previous work, a single

dx.doi.org/10.1021/nl5018145 | *Nano Lett.* 2014, 14, 4707−4714

exponential is a good approximation to the fluorescence decay traces in nanoapertures.[48,49] For the aperture diameters below 250 nm, a non-negligible background signal is detected due to the photoluminescence from the gold film excited at 550 nm and is accounted for in the lifetime analysis by adding a supplementary decay term with a fixed 5 ps characteristic time. This biexponential contribution appears more evident for 160 nm apertures (Figure 3d) or when only the acceptor is present (Figure S3b of the Supporting Information). In the case of FRET pairs with donor−acceptor separations larger than 6 nm, we also find that the single-exponential decay fits well the data. For the shortest D−A distance of 3.4 nm, the donor emission in the FRET pair is essentially quenched; consequently, we detect a relatively larger contribution from the emission of the donor when the acceptor is not fluorescing. Therefore, for this D−A distance, we add another decay term with a lifetime fixed as the isolated donor lifetime and extract only the short fluorescence lifetime contribution to quantify the FRET rate. For each aperture and each D−A separation, two sets of measurements are performed to determine the donor lifetime in the presence of the acceptor $\tau_{DA} = 1/\Gamma_{DA}$ and the donor-only lifetime in the absence of acceptor $\tau_D = 1/\Gamma_D$. The FRET efficiency is then obtained as $E_{FRET} = 1 - \Gamma_D/\Gamma_{DA} = 1 - \tau_{DA}/\tau_D$, and the FRET rate is obtained as $\Gamma_{FRET} = \Gamma_{DA} - \Gamma_D$.

FRET Analysis Based on Acceptor Fluorescence Bursts. For every detected fluorescence burst above the background noise, the number of detected photons in the acceptor channel n_a and in the donor channel n_d are recorded. Conceptually, these numbers are used to estimate the FRET efficiency as the ratio $n_a/(n_a + n_d)$ of acceptor emission events over all acceptor and donor events. Practically, several additional effects have to be taken into account to avoid experimental artifacts in the FRET analysis. These effects include the direct excitation of the acceptor by the laser light, donor emission crosstalk into the acceptor channel, and differences in the quantum yields and detection efficiencies of the donor and acceptor emission. Prior to all FRET measurements, we carefully characterize the optical response of the isolated donor and the isolated acceptor. This quantifies the number n_{ao}^{de} of photons that result from the direct excitation of the acceptor dye by the laser light. In the case of the isolated donor, we also record the fraction α of photons from the donor that fall into the acceptor detection channel due to non-negligible spectral overlap between the donor emission and the acceptor detection window. The FRET efficiency is thus computed according to the formula

$$E_{FRET} = \frac{n_a - \alpha n_d - n_{ao}^{de}}{n_a - \alpha n_d - n_{ao}^{de} + \gamma n_d} \quad (1)$$

where α is the crosstalk parameter defined as the ratio of donor-only fluorescence falling into the acceptor detection channel as compared with the donor-only signal detected in the donor channel. For all of our measurements, α is fixed to a value of 0.17; we verified that α is not affected by the nanoaperture. n_{ao}^{de} is the compensation parameter for the direct excitation of the acceptor dye by the laser light. This parameter was carefully measured for every nanoaperture by recording the average number of detected photons per burst when only the acceptor dye is present and compensating for the slight differences of concentrations between the experiments. (We use FCS to estimate the number of detected molecules and the molecular concentration in each experimental run; see the Supporting Information.) Lastly, $\gamma = \eta_a\phi_a/\eta_d\phi_d$ accounts for the differences in quantum yields (ϕ_a and ϕ_d) and fluorescence detection efficiencies (η_a and η_d) between the acceptor and donor. For the confocal reference and the nanoapertures, we estimate $\gamma = 1.3$ in the case of our setup. The full trace analysis is implemented using the software Symphotime 64 (Picoquant). From the measurement of the FRET efficiency from fluorescence bursts, we deduce the FRET rate as $\Gamma_{FRET} = \Gamma_D E_{FRET}/(1 - E_{FRET})$, where $\Gamma_D = 1/\tau_D$ is the donor-only decay rate obtained from time-correlated lifetime measurements.

■ ASSOCIATED CONTENT

Supporting Information

Fluorescence correlation spectroscopy analysis, fluorescence enhancement factors, additional fluorescence decay traces and lifetimes, FRET rates and efficiencies for large D−A separations, and discussion about the radiative and nonradiative decay rates in nanoapertures. This material is available free of charge via the Internet at http://pubs.acs.org.

■ AUTHOR INFORMATION

Corresponding Author

*E-mail: jerome.wenger@Fresnel.fr.

Notes

The authors declare no competing financial interests.

■ ACKNOWLEDGMENTS

We thank Thomas W. Ebbesen for stimulating discussions and Eloïse Devaux for help with the focused ion beam. The research leading to these results has received funding from the European Commission's Seventh Framework Programme (FP7-ICT-2011-7) under grant agreement ERC StG 278242 (ExtendFRET). P.G. is on leave from Institute for Space Sciences, Bucharest-Măgurele RO-077125, Romania.

■ REFERENCES

(1) Kühlbrandt, W.; Wang, D. N. *Nature* **1991**, *350*, 130−134.
(2) van Grondelle, R.; Dekker, J. P.; Gillbro, T.; Sundström, V. *Biochim. Biophys. Acta, Bioenerg.* **1994**, *1187*, 1−65.
(3) Hildner, R.; Brinks, D.; Nieder, J. B.; Cogdell, R. J.; van Hulst, N. F. *Science* **2013**, *340*, 1448−1451.
(4) Farrell, D. J.; Ekins-Daukes, N. J. *Nat. Photonics* **2009**, *3*, 373−374.
(5) Shankar, K.; Feng, X.; Grimes, C. A. *ACS Nano* **2009**, *3*, 788−794.
(6) Baldo, M. A.; Thompson, M. E.; Forrest, S. R. *Nature* **2000**, *403*, 750−753.
(7) Medintz, I. L.; Clapp, A. R.; Mattoussi, H.; Goldman, E. R.; Fisher, B.; Mauro, J. M. *Nat. Mater.* **2003**, *2*, 630−638.
(8) Förster, T. *Ann. Phys.* **1948**, *437*, 55−75.
(9) Roy, R.; Hohng, S.; Ha, T. *Nat. Methods* **2008**, *5*, 507−516.
(10) Weiss, S. *Nat. Struct. Biol.* **2000**, *7*, 724−729.
(11) Schuler, B.; Eaton, W. A. *Curr. Opin. Struct. Biol.* **2008**, *18*, 16−26.
(12) Purcell, E. M. *Phys. Rev.* **1946**, *69*, 681.
(13) Drexhage, K. H. *J. Lumin.* **1970**, *1*, 693−701.
(14) Novotny, L.; Hecht, B. *Principles of Nano-Optics*; Cambridge University Press: Cambridge, 2006.
(15) Barnes, W. L. *J. Mod. Opt.* **1998**, *45*, 661−699.
(16) Goy, P.; Raimond, J. M.; Gross, M.; Haroche, S. *Phys. Rev. Lett.* **1983**, *50*, 1903−1906.
(17) Yablonovitch, E. *Phys. Rev. Lett.* **1987**, *58*, 2059−2062.
(18) Lodahl, P.; Van Driel, A. F.; Nikolaev, I. S.; Irman, A.; Overgaag, K.; Vanmaekelbergh, D.; Vos, W. L. *Nature* **2004**, *430*, 654−657.
(19) Novotny, L.; van Hulst, N. *Nat. Photonics* **2011**, *5*, 83−90.

(20) Kinkhabwala, A.; Yu, Z. F.; Fan, S. H.; Avlasevich, Y.; Mullen, K.; Moerner, W. E. *Nat. Photonics* **2009**, *3*, 654−657.
(21) Hopmeier, M.; Guss, W.; Deussen, M.; Göbel, E. O.; Mahrt, R. F. *Phys. Rev. Lett.* **1999**, *82*, 4118−4121.
(22) Andrew, P.; Barnes, W. L. *Science* **2000**, *290*, 785−788.
(23) Finlayson, C. E.; Ginger, D. S.; Greenham, N. C. *Chem. Phys. Lett.* **2001**, *338*, 83−87.
(24) Nakamura, T.; Fujii, M.; Imakita, K.; Hayashi, S. *Phys. Rev. B* **2005**, *72*, 235412.
(25) Dung, H. T.; Knöll, L.; Welsch, D. G. *Phys. Rev. A* **2002**, *65*, 043813.
(26) Colas des Francs, G.; Girard, C.; Martin, O. J. *Phys. Rev. A* **2003**, *67*, 053805.
(27) Govorov, A. O.; Lee, J.; Kotov, N. A. *Phys. Rev. B* **2007**, *76*, 125308.
(28) Vincent, R.; Carminati, R. *Phys. Rev. B* **2011**, *83*, 165426.
(29) Enderlein, J. *Int. J. Mol. Sci.* **2012**, *13*, 15227−15240.
(30) Nakamura, T.; Fujii, M.; Miura, S.; Inui, M.; Hayashi, S. *Phys. Rev. B* **2006**, *74*, 045302.
(31) de Dood, M. J. A.; Knoester, J.; Tip, A.; Polman, A. *Phys. Rev. B* **2005**, *71*, 115102.
(32) Blum, C.; Zijlstra, N.; Lagendijk, A.; Wubs, M.; Mosk, A. P.; Subramaniam, V.; Vos, W. L. *Phys. Rev. Lett.* **2012**, *109*, 203601.
(33) Rabouw, F. T.; den Hartog, S. A.; Senden, T.; Meijerink, A. *Nat. Commun.* **2014**, *5*, 3610.
(34) Zhang, J.; Fu, Y.; Chowdhury, M. H.; Lakowicz, J. R. *J. Phys. Chem. C* **2007**, *111*, 11784−11792.
(35) Fore, S.; Yuen, Y.; Hesselink, L.; Huser, T. *Nano Lett.* **2007**, *7*, 1749−1756.
(36) Kolaric, B.; Baert, K.; Van der Auweraer, M.; Vallée, R. A.; Clays, K. *Chem. Mater.* **2007**, *19*, 5547−5552.
(37) Reil, F.; Hohenester, U.; Krenn, J. R.; Leitner, A. *Nano Lett.* **2008**, *8*, 4128−4133.
(38) Yang, Z.; Zhou, X.; Huang, X.; Zhou, J.; Yang, G.; Xie, Q.; Sun, L.; Li, B. *Opt. Lett.* **2008**, *33*, 1963−1965.
(39) Komarala, V. K.; Bradley, A. L.; Rakovich, Y. P.; Byrne, S. J.; Gunko, Y. K.; Rogach, A. L. *Appl. Phys. Lett.* **2008**, *93*, 123102−123102.
(40) Lunz, M.; Gerard, V. A.; Gun'ko, Y. K.; Lesnyak, V.; Gaponik, N.; Susha, A. S.; Rogach, A. L.; Bradley, A. L. *Nano Lett.* **2011**, *11*, 3341−3345.
(41) Zhang, X.; Marocico, C. A.; Lunz, M.; Gerard, V. A.; Gun'ko, Y. K.; Lesnyak, V.; Gaponik, N.; Susha, A. S.; Rogach, A. L.; Bradley, A. L. *ACS Nano* **2011**, *6*, 9283−9290.
(42) Zhang, X.; Marocico, C. A.; Lunz, M.; Gerard, V. A.; Gun'ko, Y. K.; Lesnyak, V.; Gaponik, N.; Susha, A. S.; Rogach, A. L.; Bradley, A. L. *ACS Nano* **2014**, *8*, 1273−1283.
(43) Zhao, Y.; Chen, D.; Yue, H.; Spiering, M. M.; Zhao, C.; Benkovic, S. J.; Huang, T. J. *Nano Lett.* **2014**, *14*, 1952−1960.
(44) Chen, J.; Dalal, R. V.; Petrov, A. N.; Tsai, A.; O'Leary, S. E.; Chapin, K.; Cheng, J.; Ewan, M.; Hsiung, P. L.; Lundquist, P.; Turner, S. W.; Hsu, D. R.; Puglisi, J. D. *Proc. Natl. Acad. Sci.* **2014**, *111*, 664−669.
(45) Heucke, S.; Baumann, F.; Acuna, G. P.; Severin, P. M. D.; Stahl, S. W.; Strackharn, M.; Stein, I. H.; Altpeter, P.; Tinnefeld, P.; Gaub, H. E. *Nano Lett.* **2014**, *14*, 391−395.
(46) Pibiri, E.; Holzmeister, P.; Lalkens, B.; Acuna, G. P.; Tinnefeld, P. *Nano Lett.* **2014**, *14*, 3499−3503.
(47) Rigneault, H.; Capoulade, J.; Dintinger, J.; Wenger, J.; Bonod, N.; Popov, E.; Ebbesen, T. W.; Lenne, P. F. *Phys. Rev. Lett.* **2005**, *95*, 117401.
(48) Wenger, J.; Gérard, D.; Bonod, N.; Popov, E.; Rigneault, H.; Dintinger, J.; Mahboub, O.; Ebbesen, T. W. *Opt. Express* **2008**, *16*, 3008−3020.
(49) Langguth, L.; Punj, D.; Wenger, J.; Koenderink, A. F. *ACS Nano* **2013**, *7*, 8840−8848.
(50) Deniz, A. A.; Dahan, M.; Grunwell, J. R.; Ha, T.; Faulhaber, A. E.; Chemla, D. S.; Weiss, S.; Schultz, P. G. *Proc. Natl. Acad. Sci. U. S. A.* **1999**, *96*, 3670−3675.
(51) Dolghih, E.; Roitberg, A. E.; Krause, J. L. *J. Photochem. Photobiol., A* **2007**, *190*, 321−327.
(52) Iqbal, A.; Arslan, S.; Okumus, B.; Wilson, T. J.; Giraud, G.; Norman, D. G.; Ha, T.; Lilley, D. M. *Proc. Natl. Acad. Sci. U. S. A.* **2008**, *105*, 11176−11181.
(53) Kupstat, A.; Ritschel, T.; Kumke, M. U. *Bioconjugate Chem.* **2011**, *22*, 2546−2557.
(54) Levene, M. J.; Korlach, J.; Turner, S. W.; Foquet, M.; Craighead, H. G.; Webb, W. W. *Science* **2003**, *299*, 682−686.
(55) Holzmeister, P.; Acuna, G. P.; Grohmann, D.; Tinnefeld, P. *Chem. Soc. Rev.* **2013**, *43*, 1014−1028.
(56) Punj, D.; Ghenuche, P.; Moparthi, S. B.; de Torres, J.; Grigoriev, V.; Rigneault, H.; Wenger, J. *Wiley Interdiscip. Rev.: Nanomed. Nanobiotechnol.* **2014**, *6*, 268−282.